Organic & Biomolecular Chemistry

www.rsc.org/obc

Volume 10 | Number 23 | 21 June 2012 | Pages 4473–4628

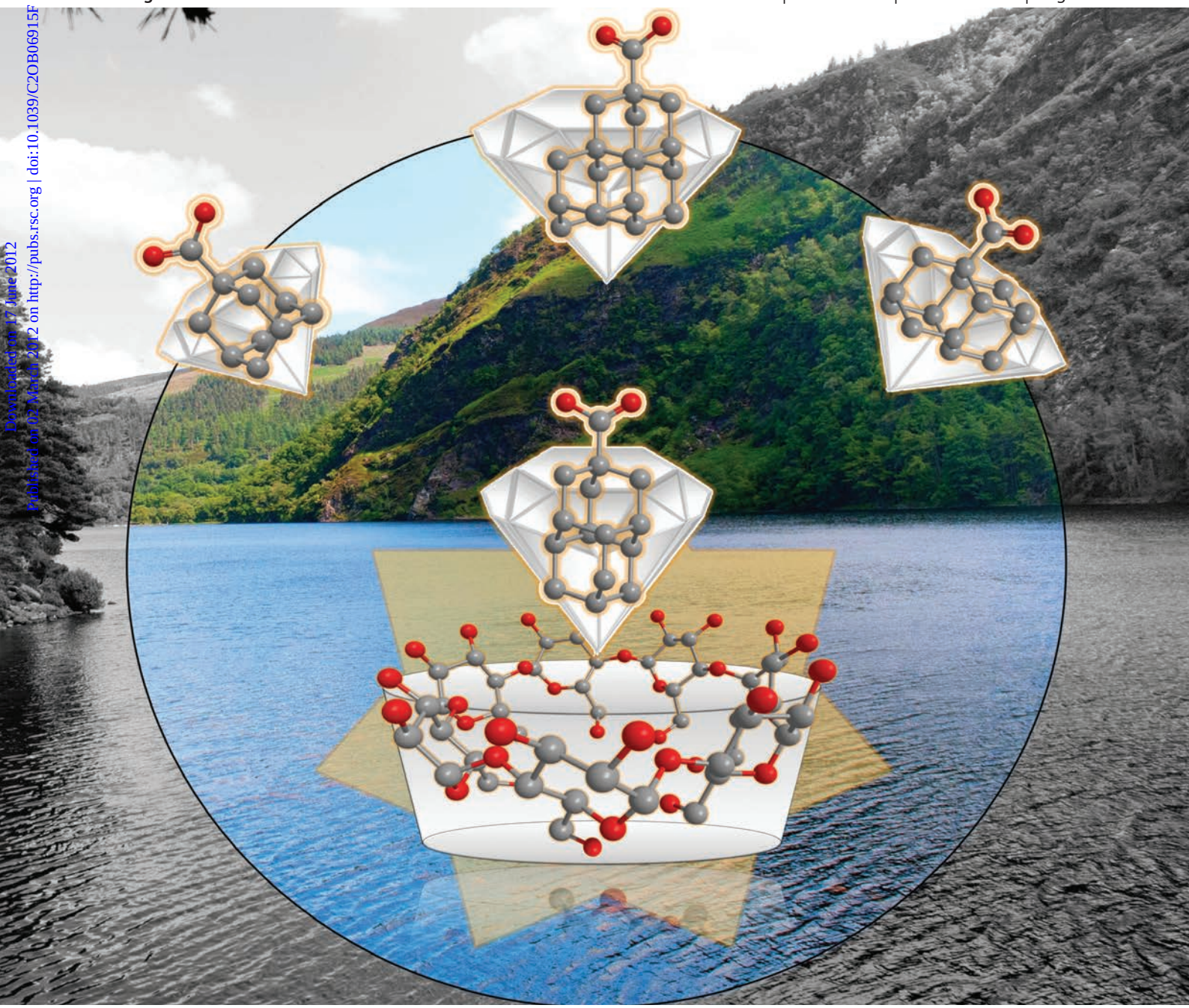

ISSN 1477-0520

RSC Publishing

PAPER

Bart Jan Ravoo *et al.*

Nanodiamonds in sugar rings: an experimental and theoretical investigation of cyclodextrin–nanodiamond inclusion complexes

Organic & Biomolecular Chemistry

Dynamic Article Links
View Online

Cite this: *Org. Biomol. Chem.*, 2012, **10**, 4524

www.rsc.org/obc

PAPER

Nanodiamonds in sugar rings: an experimental and theoretical investigation of cyclodextrin–nanodiamond inclusion complexes†

Jens Voskuhl,[a] Mark Waller,*[a] Sateesh Bandaru,[a] Boryslav A. Tkachenko,[b] Carlo Fregonese,[a] Birgit Wibbeling,[a] Peter R. Schreiner*[b] and Bart Jan Ravoo*[a]

Received 13th November 2011, Accepted 1st March 2012
DOI: 10.1039/c2ob06915f

We report on the noncovalent interactions of nanodiamond carboxylic acids derived from adamantane, diamantane, and triamantane with β- and γ-cyclodextrins. The water solubility of the nanodiamonds was increased by attaching an aromatic dicarboxylic acid *via* peptide coupling. Isothermal titration calorimetry experiments were performed to determine the thermodynamic parameters (K_a, ΔH, ΔG and ΔS) for the host–guest inclusion. The stoichiometry of the complexes is invariably 1 : 1. It was found that K_a, ΔG and ΔH of inclusion increase for larger nanodiamonds. ΔS is generally positive, in particular for the largest nanodiamonds. β-Cyclodextrin binds all nanodiamonds, γ-cyclodextrin clearly prefers the most bulky nanodiamonds. The interaction of 9-triamantane carboxylic acid shows one of the strongest complexation constants towards γ-cyclodextrin ever reported, $K_a = 5.0 \times 10^5\ M^{-1}$. In order to gain some insight into the possible structural basis of these inclusion complexes we performed density functional calculations at the B97-D3/def2-TZVPP level of theory.

Introduction

Inclusion complexes of cyclodextrins (CDs) are among the most studied host–guest pairs in supramolecular chemistry. The first examples of these non-covalent complexes were described by Pringsheim and by Freudenberg.[1,2] Nowadays, CDs are widely available *via* a cheap enzyme-catalyzed synthesis from starch. CDs have become increasingly important in a range of pharmaceutical and cosmetic applications, and they have also become valuable components of HPLC columns to separate enantiomers by stereoselective host–guest complexation.[3] In addition, CDs are key components in a variety of supramolecular materials,[4] including surfaces,[5] hydrogels,[6] and vesicles.[7]

The stability of the host–guest complexes of CDs is primarily determined by the hydrophobicity and the shape of the guest molecule and driven by the release of water molecules from the cavity of the CD into the bulk water.[3] Adamantane and ferrocene derivatives bind strongly to β-cyclodextrin (β-CD) due to their spherical shape, which nicely matches the cavity of β-CD.[8] Typical binding constants are around $K_a = 10^4\ M^{-1}$. There are few examples of 1 : 1 host–guest complexes of CDs that show higher affinity. In most of these cases, secondary interactions such as hydrogen bonding or electrostatic attraction lead to binding constants that are about one magnitude higher than those reported for adamantane and ferrocene derivatives.[9] Alternatively, large hydrophobic molecules such as steroids can be accommodated in CD dimers. In that case, the affinity can be as high as $K_a = 10^6\ M^{-1}$, but the host–guest stoichiometry is effectively 2 : 1.[10]

Inclusion complexes of γ-cyclodextrin (γ-CD) have been much less investigated. γ-CD is more flexible than β-CD. In solution, the cavity of γ-CD partially collapses and hence the tendency to replace internal hydration water with a suitable hydrophobic guest is significantly reduced. However, bulky molecules such as substituted azobenzene derivatives form strong inclusion complexes with γ-CD ($K_a > 10^4\ M^{-1}$).[11]

Diamondoids are nanometer-sized hydrocarbons (*i.e.*, nanodiamonds (NDs)) resembling the diamond lattice terminated by hydrogen atoms.[12] While adamantane ($C_{10}H_{16}$)[13] and diamantane ($C_{14}H_{20}$)[14] have long been synthetically available and therefore comprehensively studied, recent discovery of triamantane ($C_{18}H_{24}$)[15] and various higher diamondoids in oil and deep natural gas condensates[16] promoted a surge of investigations regarding their properties and applications. Diamondoids can be selectively functionalized at different positions, leading to various derivatives with unique properties that already found applications in diverse fields ranging from catalysis,[17]

[a]*Organisch Chemisches Institut, Westfälische Wilhelms-Universität Münster, Corrensstrasse 40, 48149 Münster, Germany. E-mail: b.j.ravoo@uni-muenster.de, m.waller@uni-muenster.de*
[b]*Institut für Organische Chemie, Justus-Liebig Universität, Heinrich-Buff-Ring 58, 35392 Giessen, Germany. E-mail: prs@org.chemie.uni-giessen.de*

†Electronic supplementary information (ESI) available: Synthetic procedures, NMR spectra, details of ITC measurements, coordinates of calculated complexes and a selection of geometries and energies are provided in the electronic supplementary information. CCDC 854337–854339. For ESI and crystallographic data in CIF or other electronic format see DOI: 10.1039/c2ob06915f

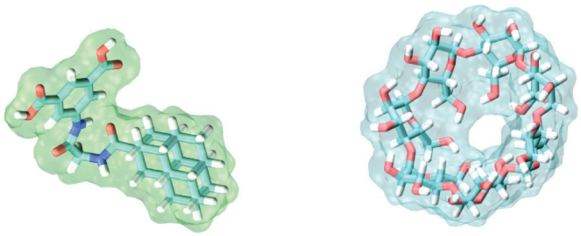

Fig. 1 Substituted nanodiamond (left) and γ-cyclodextrin (right).

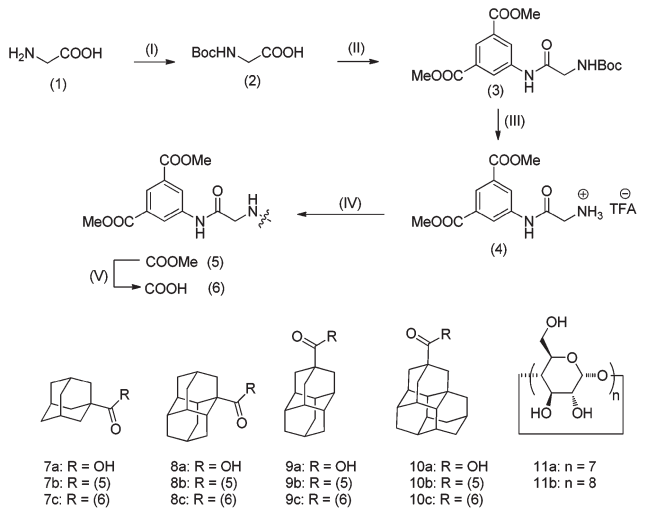

Scheme 1 Synthesis and overview of guest and host molecules. *Reagents and conditions*: (I) Boc_2O, NaOH, H_2O, *t*-BuOH, 12 h, rt, 99%, (II) EDCI, Oxyma Pure, NMM, DMF, 5-aminoisophthalic acid–dimethylester, 18 h, rt, 52%, (III) TFA, CH_2Cl_2, 4 h, rt, 99%, (IV) EDCI, Oxyma Pure, NMM, DMF, RCO_2H, 18 h, rt, 41–55%, (V) THF, MeOH, THF, Dowex HCR 20, 4 h, rt, 88–95%.

pharmaceuticals,[18] polymer science[19] to surface modification[20] and nanoelectronics.[21]

On the basis of their hydrophobicity and symmetry, it would be expected that NDs are excellent guests for β-CD and γ-CD (Fig. 1). To the best of our knowledge, the host–guest interactions of CDs and NDs have not been investigated before. The aim of this study is to characterize the inclusion complexes of the lower NDs with β-CD and γ-CD. To this end, we determined the thermodynamic parameters (association constant K_a, enthalpy ΔH, free energy ΔG and entropy ΔS) for the inclusion complexation of 1-adamantane, 1-diamantane, 4-diamantane and 9-triamantane carboxylic acids by isothermal titration calorimetry (ITC). We also prepared a range of hydrophilic derivatives of the NDs by peptide coupling with 5-aminoisophthalic acid (Scheme 1). The inclusion of these NDs was also characterized by ITC. It should be emphasized that both the ND carboxylic acids and their isophthalic acid derivatives may show secondary interaction with CDs through hydrogen bonding, resulting in additional stabilization of the inclusion complex. However, we do not expect inclusion of the hydrophilic aromatic substituent in the CD cavity.

In order to gain some insight into the possible structural basis of these inclusion complexes we also performed density functional theory (DFT) computations. An exhaustive review on the application of force fields for studying CDs was published by Lipkowitz in 1998.[22] The use of empirical potentials to model the CD was primarily due to the limited computing resources at that time. Since then, advances in computing hardware and computational techniques have opened up a new vista of accuracy for modelling CD complexes. DFT is often referred to as the "workhorse" of quantum chemistry, and due to its accuracy and favorable scaling properties it has become widely used to study CD complexes. For example, Snor *et al.* published a series of papers on the structure of anhydrous CDs,[23–25] including complexes with spironolactone[26] and meloxicam.[27] Furthermore, Rarati *et al.* investigated decyltrimethylammonium bromide (DTAB) and tetradecyltrimethylammonium bromide (TTAB) inclusion complexes with α-CD and β-CD using semi-empirical and DFT computations.[28] The binding affinities of resorcinol and a series of drugs (flubiprofen, nabumetone and naproxen) with CDs showed good agreement between classical simulations and experimental values.[29]

It should be noted that in the gas phase the binding of an adamantane moiety will be predominately a result of dispersion type interactions while in solution hydrophobic interactions will dominate. The inability of most available functionals to describe van der Waals type interactions is a topic of current research. Furthermore, a cursory consideration of structure of the substituted NDs shows that the ligands may form an additional hydrogen bonding interaction *via* the attached isophthalic acid. Therefore, a modelling method that is capable of delivering an accurate and balanced description of dispersion bound and hydrogen bound complexes is required. In this study, we will use B97 density functional that is augmented with a third generation dispersion correction, denoted D3,[30] which has been shown recently to perform well in benchmark studies.[31]

Methods and results

Synthesis

The carboxylic acids of diamantane and triamantane were synthesized as described before.[32] The synthesis of the substituted nanodiamonds starts from glycine **1** which was first amine protected followed by peptide coupling using EDCI, NMM and Oxyma Pure (ethyl 2-cyano-2-(hydroxyimino)acetate) to 5-aminoisophthalic acid methylester yielding **2**. After removal of the protection group using TFA and coupling of the free amine to the diamondoid carboxylic acids **7a–10a** the protected guest molecules **7b–10b** were obtained. The final step was a saponification with sodium hydroxide followed by neutralization with ion exchange resin (HWCR-20) yielding the desired highly water soluble nanodiamonds **7c–10c**.

The analytical data of **7b–10c** are consistent with their molecular structure. Details are available as electronic supplementary information (ESI†). It was possible to obtain X-ray structures of compounds **7b, 8b** and **10b**, which confirm the diamondoid structures (Fig. 2). It is evident that the compounds contain the compact hydrophobic NDs linked to **3** *via* a peptide bond.

Isothermal titration calorimetry (ITC)

With guest molecules **7b–10c** in stock it was possible to investigate their ability of forming inclusion complexes with β- and

γ-cyclodextrins. With exception of **10c**, the NDs were titrated to the CDs. Table 1 presents an overview of the ITC data; details are available as ESI.† All NDs interact with β-CD, but only the bulkiest ones (**8c, 10a, 10c**) interact with γ-CD. The stoichiometry is 1 : 1 and the interaction is endothermic in each case, with increasingly negative ΔH for the larger NDs. No significant enthalpy change was detected for the titrations of **7a, 7c, 8a, 9a** and **9c** to γ-CD. Compared to the complexes of β-CD, the complexes of γ-CD have a much smaller ΔH and much larger ΔS.

Computational details

Hereafter, we use the nomenclature ND·*x*-CD, where ND indicates the guest, and *x* can be either β or γ. Therefore, we have four possible ND·β-CD and four possible ND·γ-CD. We note that the adamantane typically binds end-on,[33] in contrast to the prototypical threaded binding motif of rotaxane. Therefore we performed a series of calculations where the adamantane entered the larger secondary face (S), and a series where the narrower primary face (P) is penetrated. Gas-phase structural optimizations were undertaken with the B97-D3[34] method combined with the def-SV(P)[35] basis set using the TURBOMOLE 6.3[36] suite. An overview of energetic and descriptors is provided in Table 2.[37] Subsequently, single point energies were computed at the B97-D3[30]/def2-TZVPP for binding and deformation energies. The degree of penetration for the ND·CD complexes is presented as the distance, R_p, defined as the distance between the centre-of-mass (COM) of the CD and the COM of the adamantane subunit that is the closest to the CD COM. To quantify the tilt angle of the guest molecule with respect to the CD, we present the angle (θ) between CD_{COM}–ND_{COM}–C_{linker} in Table 2. The system specific density functional validation results are given in the ESI.† We have validated our functional selection from amongst four popular gradient corrected functionals (GGA). They show a small functional dependence across the small model systems of our ND·*x*-CD systems.

Solvation effects were modelled using a 17 Å sphere of TIP3P[38] water molecules centred on the COM of the ND (~1800 atoms). A QM/MM strategy was employed whereby the gas-phase optimized NDs **7b–10c** and CDs were both assigned to the QM layer and the solvation sphere was assigned to the MM layer (Charmm C35ba[39]). The Chemshell v3.3.2 package[40] was employed for the QM/MM energy minimization at the B97-D3/def-SV(P):CHARMM level of theory. A root mean square distortion (RMSD) overlay was performed within the VMD visualization package.[41]

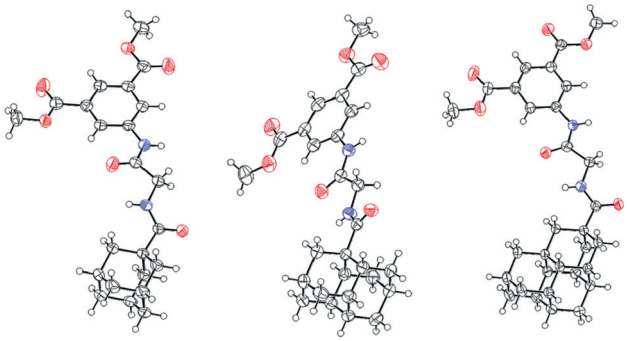

Fig. 2 X-ray structure of **7b, 8b** and **10b**. Thermal ellipsoids indicate 50% probability.

Discussion

The diameter of the CD cavity increases as the number of α-D-glucopyranoside units are increased from six (α-CD) to seven (β-CD) to eight (γ-CD). When the rim of the CD is penetrated by the adamantane, the CD can increase its interstitial diameter to accommodate the ND ligand. We note that there is a larger degree of distortion, *i.e.*, higher RMSD, for the DFT optimized γ-CDs models than for the β-CD counterparts (Table 2). This distortion can be traced back to the increased ellipticity of the γ-CD that is required to envelope the guest molecules, thereby maximizing close contacts (Fig. 3).

Table 1 Thermodynamic parameters of the host–guest complexation between nanodiamonds (NDs) and cyclodextrins (CDs) obtained by isothermal titration calorimetry

Nr	ND	Guest	Host	[Guest] (mM)	[Host] (mM)	ΔH (kJ mol^{-1})	ΔG (kJ mol^{-1})	ΔS (J kmol^{-1})	K_a (M^{-1}) 10^4
A	1-Adamantane	**7a**	β-CD	10.0	1.0	−17.8	−24.8	23.6	2.2
B		**7a**	γ-CD	10.0	1.0	—[a]	—[a]	—[a]	—[a]
C		**7c**	β-CD	10.0	1.0	−17.3	−24.6	24.4	2.0
D		**7c**	γ-CD	10.0	1.0	—[a]	—[a]	—[a]	—[a]
E	1-Diamantane	**8a**	β-CD	1.0	0.1	−21.9	−29.1	24.1	12.8
F		**8a**	γ-CD	10.0	1.0	—[a]	—[a]	—[a]	—[a]
G		**8c**	β-CD	10.0	1.0	−25.1	−26.3	4.2	4.1
H		**8c**	γ-CD	10.0	1.0	−4.9	−26.2	71.3	3.9
I	4-Diamantane	**9a**	β-CD	10.0	1.0	−22.8	−30.3	25.3	20.7
J		**9a**	γ-CD	10.0	1.0	—[a]	—[a]	—[a]	—[a]
K		**9c**	β-CD	10.0	1.0	−20.1	−31.1	37.0	28.7
L		**9c**	γ-CD	10.0	1.0	—[a]	—[a]	—[a]	—[a]
M	9-Triamantane	**10a**	β-CD	1.0	0.1	−34.9	−29.5	−18.4	14.7
N		**10a**	γ-CD	5.0	0.5	−8.7	−32.5	80.0	50.0
O[b]		**10c**	β-CD	1.0	10.0	−35.7	−24.8	−36.3	2.3
P[b]		**10c**	γ-CD	1.0	10.0	−11.3	−31.9	69.1	39.1

[a] No detectable signals were obtained during ITC measurements. [b] Due to micelle formation, the titration was performed in the inverse mode.

Table 2 The gas-phase energetics of nanodiamond (ND)·cyclodextrin (CD) complexes at the B97-D3/def2-TZVPP level of theory, and the structural descriptors of ND·CD complexes that were optimized at the B97-D/def-SV(P) level of theory

Nr	ND	Guest	Host	BE (kJ mol^{-1})	DE^{CD} (kJ mol^{-1})	DEND (kJ mol^{-1})	RMSD^{CD} (Å)	RMSDND (Å)	Rp (Å)	Pept (ψ)	Tilt (θ)
A	1-Adamantane	**7a**	β-CD	−77	33	6	0.52	0.69	1.2	—	124
B		**7a**	γ-CD	−134	20	38	1.67	0.19	1.2	—	23
C		**7c**	β-CD	−135	85	40	0.65	2.88	0.8	80	141
D		**7c**	γ-CD	−117	−1	17	0.91	2.72	0.3	27	136
E	1-Diamantane	**8a**	β-CD	−84	41	9	0.56	0.18	1.8	—	126
F		**8a**	γ-CD	−142	−23	13	0.83	2.62	1.2	—	110
G		**8c**	β-CD	−97	48	2	0.52	1.59	2.6	−176	141
H		**8c**	γ-CD	−183	10	56	0.89	4.35	1.5	−37	156
I	4-Diamantane	**9a**	β-CD	−32	75	−2	1.49	0.24	1.7	—	138
J		**9a**	γ-CD	−161	7	19	1.51	2.65	2.1	–	14
K		**9c**	β-CD	−82	79	13	1.29	1.65	0.9	68	154
L		**9c**	γ-CD	−233	−1	68	1.15	3.58	0.9	76	36
M	9-Triamantane	**10a**	β-CD	−121	21	19	0.48	0.51	1.5	—	105
N		**10a**	γ-CD	−172	−31	11	1.18	2.59	1.2	—	144
O		**10c**	β-CD	−125	15	12	0.46	2.92	1.4	69	108
P		**10c**	γ-CD	−250	−24	17	1.42	4.39	0.6	61	142

Note: only the complexes where the secondary side of the CD ring was penetrated by the ligands are shown in above. Table S1 (ESI†) contains the corresponding data for the primary complex.

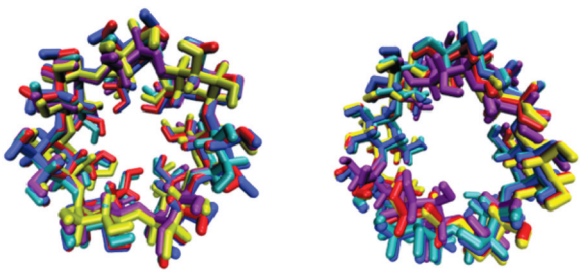

Fig. 3 (a) The overlaid β-CDs taken from the optimized complexes (NDs removed for clarity), of note is the circular cavity. (b) The overlaid γ-CD taken from the optimized complexes (ND removed for clarity). Note the elliptical distortion resulting from the bound **ND**, especially for the **7c**·γ-**CD** (purple).

1-Adamantane

The association constant K_a for the interaction of **7a** and **7c** with β-CD was found to be around 2.0×10^4 M^{-1}. No significant ΔH was determined for the titration of **7a** and **7c** with γ-CD.[42] It is intriguing that the isophthalic acid substituent does not cause a decrease or increase in binding constant or have any significant influence on other thermodynamic parameters. This similarity is not borne out in the DFT optimized structures where a nearly two-fold increase in binding energy is observed (BE, Table 2). This large difference is associated with a dramatic decrease in the distance (R_p) between the shallow bound nonsubstituted **7a**·β-CD complex and the deeply bound substituted **7c**·β-CD complex. There is a rather small difference in BE between the ND that is complexed with the S side of the CD in Table 2, compared to binding at the P side (see Table S1 in the ESI†). Therefore, although thermodynamically the preference is not that large in the gas phase, binding *via* the narrow P side of the CD is far less likely than *via* the wider S side. Either the ND has to push the entire hydrophilic carboxylic acid group(s) through the centre of the hydrophobic CD core to penetrate through to the P side. Alternatively, one could imagine the ND penetrating the narrow P side with the entire bulky ND, with the acid group(s) anchoring the insertion process; this obviously results in a large structural deformation of the CD. Both of these insertion scenarios would be associated with a substantial kinetic barrier to insertion. For these reasons, we only show the computations with the ND bound to the S side of the CD in Table 2. All of the computational results presented in Table 2 are gas phase values. To ensure our geometries were still reasonable, given that the ITC experiments are performed in an aqueous environment, we performed an explicit solvation computation. A hybrid QM/MM method wherein the complex was assigned to the QM layer and the solvent was placed in the MM layer. The smallest substituted ND was chosen (**7c**) in conjunction with γ-CD, which has a larger cavity than β-CD. Although there was no observed interaction *via* ITC, we believe that looking at this particular complex is instructive to ascertain the effects of explicit solvation. The optimized conformation of the complex is not significantly altered (RMSD of only 0.4 Å) by the inclusion of ~1800 explicit solvent water molecules (Fig. 4). The small changes with the inclusion of solvent are in agreement with previous finding by Miyamoto *et al.*[43] for coenzyme Q_{10} complexed with γ-CD. However, we do note that the effect of explicit solvation was found to be critical when Jamie *et al.* investigated CDs with MD simulations, and care should therefore be taken when modelling in the gas-phase.

1-Diamantane

The interaction of ND **8a** with β-CD shows a remarkably high affinity of $K_a = 1.2 \times 10^5$ M^{-1}. The oblate shape and larger volume of the ND is somewhat complimentary to the cavity of the β-CD, as evidenced by an extremely small RDSDND of 0.18 Å (Table 2). Furthermore, in the DFT gas-phase optimizations of **8a**·β-CD, the complex is ~7 kJ mol^{-1} more stable than the respective **7a**·β-CD complex and these two factors combine to explain the enhanced binding affinity of 1-diamantane in comparison with the 1-adamantane carboxylic acid **7a**. Interestingly

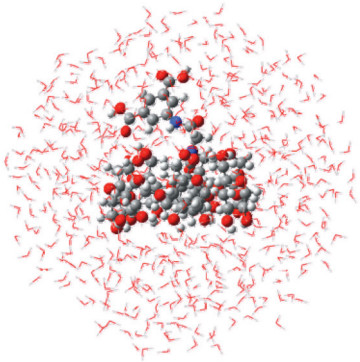

Fig. 4 Explicitly solvated QM/MM model of **7c**·γ-CD.

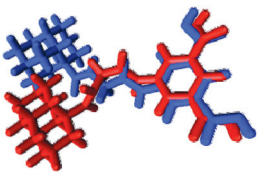

Fig. 5 *cis–trans* Isomerization of the glycine peptide bond for **8c**. *cis* (red) and *trans* (blue) Isomers are shown.

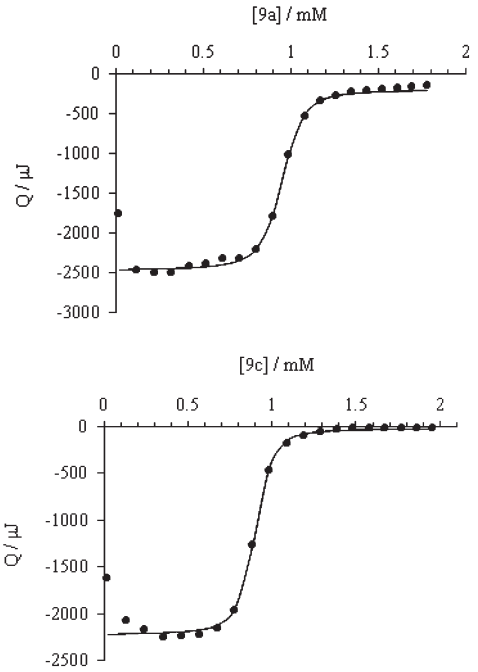

Fig. 6 Isothermal titration calorimetry of **9a** and **9c** with β-cyclodextrin. For concentrations and thermodynamic parameters see Table 1.

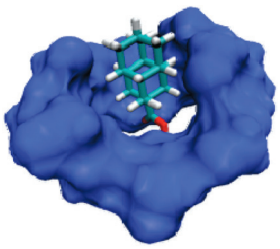

Fig. 7 Nanodiamond **9a** occupying the P opening of β-cyclodextrin.

the binding affinity decreases significantly upon substitution of the acid functionality of the ND (K_a = 4.1 × 10^4 M^{-1} for **8c**). It is possible that the hydrophilic and bulky isophthalic acid suppresses the complete insertion of the guest molecule in the cavity. Nevertheless, the interaction of **8c** and β-CD is substantial. Two possible scenarios can explain this. The first possibility is that the isophthalic acid sticks up (perpendicularly) out of the CD cavity into solvent bulk and does not have any influence. Alternatively, the carboxylic acid of **8a** can itself form a hydrogen bond with the CD rim that is effectively isoenergetic with the hydrogen bonding ability of the carboxylic acid of the isophthalic acid group of **8c**. The DFT optimized structures (and to some extent energetics) for the gas-phase **8a**·β-CD and **8c**·β-CD complexes certainly suggests that the second scenario occurs. The DFT optimizations show that the NDs lie inside the bowl shaped interior of the CDs as observed by the tilt angle (θ), which is significantly distorted away from linearity, and this tilt is more acute than observed for the isophthalic ND derivative **8c**.

Furthermore, in spite of a substantial affinity (K_a = 3.9 × 10^4 M^{-1}) for the complexation of **8c** with γ-CD, the experimental ΔH value is surprisingly small at only −4.9 kJ mol^{-1}. A large positive ΔS value of +71.3 J K^{-1} mol^{-1} observed with ITC suggests that the disorder in the system increases and the complexation is no longer primarily driven by enthalpy but by entropy instead. The release of water molecules from the CD cavity as well as a release of hydration water from the guest molecules indicates a significant penetration of the ND into the CD cavity. Indeed the DFT gas-phase optimized geometry confirms this (R_p = 1.5 Å) showing the long flexible linker forming a stabilizing hydrogen bond to the CD rim. The DFT optimized models of **8c** suggest that there is rotation about the peptide bond (Fig. 5). This is in stark contrast to **8a**, which shows no detectable complexation with γ-CD.

4-Diamantane

The 4-diamantane carboxylic acid **9a** reveals one of the strongest binding constants towards β-CD ever reported for a 1 : 1 complex: K_a = 2.1 × 10^5 M^{-1}. Representative ITC results are shown in Fig. 6. Based on the tubular, prolate structure of the ND, the hydrophobic guest can penetrate the β-CD cavity and effectively occupy this void (Fig. 7). If the ND ligand has the hydrophilic isophthalic acid substituent (**9c**) the binding is even stronger (K_a = 2.8 × 10^5 M^{-1}). Based on the small differences in enthalpy, see Table 1, we speculate that this enhanced binding affinity is due to the **9c**·ND sitting more deeply in the CD cavity. Indeed the R_p obtained from modeling is rather low at 0.9 Å, which indicates significant penetration, and therefore, *ipso facto*, a significant number of water molecules are displaced from the CD cavity into the bulk.

As expected NDs **9a** and **9c** show no significant complexation with γ-CD due to their reduced girth compared to 1-diamantane, *i.e.*, they possess a cross section more comparable to 1-adamantane. This is clearly reflected in the gas phase models where the γ-CD secondary rim must dramatically distort away from its minima (circular), to form an elliptical shaped cavity in order to

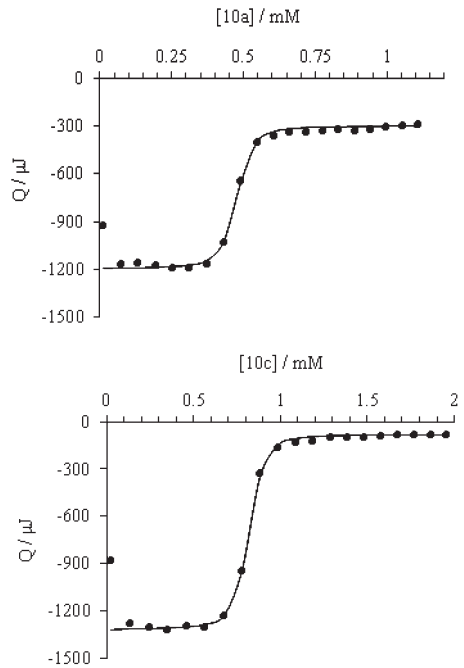

Fig. 8 Isothermal titration calorimetry of **10a** and **10c** with γ-cyclodextrin. For concentrations and thermodynamic parameters see Table 1.

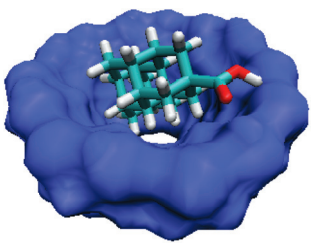

Fig. 9 Nanodiamond **10a** lying in the γ-cyclodextrin cavity forming hydrogen bonds to the cyclodextrin rim.

increase possible interactions with the ND located in its centre. The γ-CD cavity is simply too large to bind the slim 4-diamantane tube.

9-Triamantane

It is expected that triamantanes **10a** and **10c** should have a substantial affinity for CDs due to their bulky hydrophobic structure. Indeed triamantane **10a** forms the strongest ever reported inclusion complex with γ-CD for a 1 : 1 complexation (K_a = 5.0 × 10^5 M^{-1}). ND **10a** also binds to β-CD, but weaker than to γ-CD (K_a = 1.5 × 10^5 M^{-1}). Representative ITC results are shown in Fig. 8. This reduced binding affinity is evidently due to the high deformation energy required to expand the smaller β-CD cavity to accommodate the bulky triamantane group ($RMSD^{CD}$ = 0.45 Å and R_p = 1.6 Å). The hydrogen bonding network of β-CD[44] is presumably destroyed by such significant distortions. This observed expansion is in stark contrast to the **9a**·γ-CD case (see above) where the γ-CD must contract and become elliptically distorted. The 9-triamantane structure should form a strong complex with γ-CD and should also give a strong complex with β-CD. The larger volume of ND **10a** is in good agreement with the space-filling model of the hydrophobic γ-CD cavity. Fig. 9 shows ND **10a** nicely occupies the γ-CD bowl-shaped cavity, with the carboxylic acid clearly pointing towards the secondary rim forming strong hydrogen bonds.

The ITC results reveal that the interaction of the triamantanes with γ-CD is both enthalpically and entropically highly favourable. The highly positive entropy of inclusion confirms a deep penetration of the NDs into the γ-CD cavity, with concomitant release of hydration water. On the other hand, the interaction of the triamantanes with β-CD is no longer entropically favourable, which indicates that the hydrophobic part does not penetrate the cavity completely. The substituent on the triamantane cage also influences the complexation. The K_a value for the β-CD complexation decreases by a factor of six for ND **10c** in comparison with ND **10a**. However, the isophthalic acid substituent on ND **10c** does not lead to a substantial decrease of the binding constant (3.9 × 10^5 M^{-1}) for the complex with γ-CD.

Conclusion

Herein we have investigated a new class of host–guest complexes using a combined experimental and theoretical approach. ITC revealed very strong interactions between the 4-diamantanes and β-CD. Triamantane shows the highest affinity towards complexation with γ-CD ever reported. Computational studies provided some insights into the structure of the inclusion complexes. Proposed structures are based on a careful inspection of the gas phase as well as explicitly solvated models of the ND·CD complexes. The adamantane moiety of the ND occupies the CD cavity, and upon rotation of the glycine linker, secondary hydrogen bonding can occur between the carboxyl group and the CD rim. Our findings consistently indicate that an optimal fit of host and guest results in the most stable inclusion complexes.

Acknowledgements

Cyclodextrins were kindly donated by Wacker Chemie AG. The Deutsche Forschungsgemeinschaft (grants Ra 1732/1-1 to BJR, Schr 597/12-1 to PRS and SFB 858 to MW) are acknowledged for financial support.

Notes and references

1 H. Pringsheim, *Ber. Dtsch. Chem. Ges.*, 1913, **46**, 2959–2974.
2 K. Freudenberg and F. Cramer, *Chem. Ber.*, 1950, **83**, 296–304.
3 For an overview of the chemistry and applications of cyclodextrins, see: (*a*) *Chem. Rev.*, 1998, **98**, 1741–2076 (special issue on cyclodextrins); (*b*) *Cyclodextrins and Their Complexes*, ed. H. Dodziuk, Wiley-VCH, 2006.
4 (*a*) A. Mulder, J. Huskens and D. N. Reinhoudt, *Org. Biomol. Chem.*, 2004, **2**, 3409–3424; (*b*) G. Chen and M. Jiang, *Chem. Soc. Rev.*, 2011, **40**, 2254–2266.
5 (*a*) M. T. Rojas, R. Koniger, J. F. Stoddart and A. E. Kaifer, *J. Am. Chem. Soc.*, 1995, **117**, 336–343; (*b*) X. Y. Ling, D. N. Reinhoudt and J. Huskens, *Chem. Mater.*, 2008, **20**, 3574–3578; (*c*) M. D. Yilmaz, S. H. Hsu, D. N. Reinhoudt, A. H. Velders and J. Huskens, *Angew. Chem., Int. Ed.*, 2010, **49**, 5938–5941.
6 (*a*) I. Tomatsu, A. Hashidzume and A. Harada, *Macromolecules*, 2005, **38**, 5223–5227; (*b*) A. Harada, R. Kobayashi, Y. Takashima, A. Hashidzume and H. Yamaguchi, *Nat. Chem.*, 2011, **3**, 34–37.

7 (*a*) J. Voskuhl, M. C. A. Stuart and B. J. Ravoo, *Chem.–Eur. J.*, 2010, **16**, 2790–2796; (*b*) S. K. M. Nalluri, J. Voskuhl, J. L. Bultema, E. J. Boekema and B. J. Ravoo, *Angew. Chem., Int. Ed.*, 2011, **50**, 9747–9751.
8 (*a*) B. Zhang and R. Breslow, *J. Am. Chem. Soc.*, 1993, **115**, 9354–9354; (*b*) M. Weickenmeier and G. Wenz, *Macromol. Rapid Commun.*, 1996, **17**, 731–736; (*c*) L. A. Godinez, K. Saeki, S. Patel, C. M. Criss and A. E. Kaifer, *J. Phys. Chem.*, 1995, **99**, 17449–17455.
9 K. Kano, R. Nishiyabu and R. Doi, *J. Org. Chem.*, 2005, **70**, 3667–3673.
10 (*a*) M. R. de Jong, J. F. J. Engbersen, J. Huskens and D. N. Reinhoudt, *Chem.–Eur. J.*, 2000, **6**, 4034–4040; (*b*) Y. Liu, Y. W. Yang, E. C. Yang and X. D. Guan, *J. Org. Chem.*, 2004, **69**, 6590–6602.
11 A. F. D. Denamor, R. Traboulssi and D. F. V. Lewis, *J. Am. Chem. Soc.*, 1990, **112**, 8442–8447.
12 H. Schwertfeger, A. A. Fokin and P. R. Schreiner, *Angew. Chem., Int. Ed.*, 2008, **47**, 1022–1036.
13 P. von R. Schleyer, *J. Am. Chem. Soc.*, 1957, **79**, 3292–3292.
14 C. Cupas, P. v. R. Schleyer and D. J. Trecker, *J. Am. Chem. Soc.*, 1965, **87**, 917–918.
15 V. Z. Williams, P. von R. Schleyer, G. J. Gleicher and L. B. Rodewald, *J. Am. Chem. Soc.*, 1966, **88**, 3862–3863.
16 J. E. P. Dahl, S. G. Liu and R. M. K. Carlson, *Science*, 2003, **299**, 96–99.
17 H. Richter, H. Schwertfeger, P. R. Schreiner, R. Fröhlich and F. Glorius, *Synlett*, 2009, 193–197.
18 A. A. Fokin, A. Merz, N. A. Fokina, H. Schwertfeger, S. H. Liu, J. E. P. Dahl, R. K. M. Carlson and P. R. Schreiner, *Synthesis*, 2009, 909–912.
19 C. Sinkel, S. Agarwal, N. A. Fokina and P. R. Schreiner, *J. Appl. Polym. Sci.*, 2009, **114**, 2109–2115.
20 (*a*) T. M. Willey, J. D. Fabbri, J. R. I. Lee, P. R. Schreiner, A. A. Fokin, B. A. Tkachenko, N. A. Fokina, J. E. P. Dahl, R. M. K. Carlson, A. L. Vance, W. Yang, L. J. Terminello, T. van Buuren and N. A. Melosh, *J. Am. Chem. Soc.*, 2008, **130**, 10536–10544; (*b*) T. M. Willey, R. I. L. Jonathan, J. D. Fabbri, D. Wang, M. H. Nielsen, J. C. Randel, P. R. Schreiner, A. A. Fokin, B. A. Tkachenko, N. A. Fokina, J. E. P. Dahl, R. M. K. Carlson, L. J. Terminello, N. A. Melosh and T. van Buuren, *J. Electron Spectrosc. Relat. Phenom.*, 2009, **172**, 69.
21 (*a*) W. L. Yang, J. D. Fabbri, T. M. Willey, J. R. I. Lee, J. E. P. Dahl, R. M. K. Carlson, P. R. Schreiner, A. A. Fokin, B. A. Tkachenko, N. A. Fokina, W. Meevasana, N. Mannella, K. Tanaka, X. J. Zhou, T. van Buuren, M. A. Kelly, Z. Hussain, N. A. Melosh and Z. X. Shen, *Science*, 2007, **316**, 1460–1462; (*b*) W. A. Clay, Z. Liu, W. Yang, J. D. Fabbri, J. E. P. Dahl, R. M. K. Carlson, Y. Sun, P. R. Schreiner, A. A. Fokin, B. A. Tkachenko, N. A. Fokina, P. A. Pianetta, N. A. Melosh and Z. X. Shen, *Nano Lett.*, 2009, **9**, 57–61; (*c*) S. Roth, D. Leuenberger, J. Osterwalder, J. E. P. Dahl, R. M. K. Carlson, B. A. Tkachenko, A. A. Fokin, P. R. Schreiner and M. Hengsberger, *Chem. Phys. Lett.*, 2010, **495**, 102–108.
22 K. B. Lipkowitz, *Chem. Rev.*, 1998, **98**, 1829–1873.
23 A. Karpfen, E. Liedl, W. Snor and P. Wolschann, *J. Inclusion Phenom. Macrocyclic Chem.*, 2007, **57**, 35–38.
24 W. Snor, E. Liedl, P. Weiss-Greiler, A. Karpfen, H. Viernstein and P. Wolschann, *Chem. Phys. Lett.*, 2007, **441**, 159–162.
25 A. Karpfen, E. Liedl, W. Snor, H. Viernstein and P. Weiss-Greiler, *Monatsh. Chem.*, 2008, **139**, 363–371.
26 P. Weinzinger, P. Weiss-Greiler, W. Snor, H. Viernstein and P. Wolschann, *J. Inclusion Phenom. Macrocyclic Chem.*, 2007, **57**, 29–33.
27 W. Snor, E. Liedl, P. Weiss-Greiler, H. Viernstein and P. Wolschann, *Int. J. Pharm.*, 2009, **381**, 146–152.
28 A. A. Rafai, S. M. Hashemianzadeh, Z. B. Nojini and M. A. Safarpour, *J. Mol. Liq.*, 2007, **135**, 153–157.
29 W. Chen, C. E. Chang and M. K. Gilson, *Biophys. J.*, 2004, **87**, 3035–3049.
30 S. Grimme, J. Antony, S. Ehrlich and H. Krieg, *J. Chem. Phys.*, 2010, **132**, 154104.
31 L. Goerigk and S. Grimme, *J. Chem. Theory Comput.*, 2011, **7**, 291–309.
32 (*a*) T. M. Gund, M. Nomura and P. v. R. Schleyer, *J. Org. Chem.*, 1974, **39**, 2987–2994; (*b*) N. A. Fokina, B. A. Tkachenko, J. E. P. Dahl, R. M. K. Carlson, A. A. Fokin and P. R. Schreiner, *Synthesis*, 2012, 259–264.
33 See for example:M. Rekharsky and Y. Inoue, *Chem. Rev.*, 1998, **98**, 1875–1917.
34 S. Grimme, *J. Comput. Chem.*, 2004, **25**, 1463–1473.
35 A. Schaefer, H. Horn and R. Ahlrichs, *J. Chem. Phys.*, 1992, **97**, 2571.
36 TURBOMOLE V6.2 2010, a development of University of Karlsruhe and Forschungszentrum Karlsruhe GmbH, 1989–2007, TURBOMOLE GmbH, since 2007; available from http://www.turbomole.com
37 To ensure our results are not biased due to our rather small basis set, further selected models were re-optimized at the B97-D[29] GGA functional def2-TZVPP[35] level of theory. This level of theory was shown to be an excellent method in a recent benchmark study on related systems.[31] The RMSD for selected models is only 0.2 Å, with the only notable difference being a slightly shorter distance between the carboxylic acid of the substituent and the rim of the CD, this was due to slight distortion away from planarity.
38 W. L. Jorgensen, J. Chandrasekhar, J. D. Madura, R. W. Impey and M. L. Klein, *J. Chem. Phys.*, 1983, **79**, 926–935.
39 B. R. Brooks, C. L. Brooks III, A. D. Mackerell, L. Nilsson, R. J. Petrella, B. Roux, Y. Won, G. Archontis, C. Bartels, S. Boresch, A. Caflisch, L. Caves, Q. Cui, A. R. Dinner, M. Feig, S. Fischer, J. Gao, M. Hodoscek, W. Im, K. Kuczera, T. Lazaridis, J. Ma, V. Ovchinnikov, E. Paci, R. W. Pastor, C. B. Post, J. Z. Pu, M. Schaefer, B. Tidor, R. M. Venable, H. L. Woodcock, X. Wu, W. Yang, D. M. York and M. Karplus, *J. Comput. Chem.*, 2009, **30**, 1545–1615.
40 P. Sherwood, A. H. de Vries, M. F. Guest, G. Schreckenbach, C. R. A. Catlow, S. A. French, A. A. Sokol, S. T. Bromley, W. Thiel, A. J. Turner, S. Billeter, F. Terstegen, S. Thiel, J. Kendrick, S. C. Rogers, J. Casci, M. Watson, F. King, E. Karlsen, M. Sjøvoll, A. Fahmi, A. Schäfer and Ch. Lennartz, *THEOCHEM*, 2003, **632**, 1–28.
41 W. Humphrey, A. Dalke and K. Schulten, *J. Mol. Graphics*, 1996, **14**, 33–38.
42 It has been reported that **7a** forms a complex with γ-CD, however the ΔH of complexation is rather small:W. C. Cromwell, K. Bystrom and M. R. Efting, *J. Phys. Chem.*, 1985, **89**, 326–332.
43 S. Miyamoto, A. Kawai, S. Higuchi, Y. Nishi, T. Tanimoto, Y. Uekaji, D. Nakata, H. Fukumi and K. Terao, *Chem-Bio Inf. J.*, 2009, **9**, 1–11.
44 W. Saenger, C. B. V. Zabel, G. M. Brown, B. E. Hingerty, B. Lesyng and S. A. Mason, *Proc. Int. Symp. Biomol. Struct. Interact., Suppl. J. Biosci.*, 1985, **8**, 437–450.

